NEAR SURFACE METEOROLOGICAL MEASUREMENTS IN THE VICINITY OF A SCRAP-IRON RECYCLING FACTORY IN SOUTHWESTERN NIGERIA

Supported by tetfund TERTIARY EDUCATION TRUST FUND

O. E. Abiye[1]*, L. A. Sunmonu[2], M. A. Ayoola[2], A. I. Ajao[2], O. E.Akinola[2,3] and O. A. Babatunde[2]
[1]Centre for Energy Research & Development, Obafemi Awolowo University, Ile-Ife, Nigeria
[2]Atmospheric Physics Research Group, Department of Physics & Engineering Physics, Obafemi Awolowo University, Ile-Ife, Nigeria
[3]Key Laboratory for Aerosol-Cloud-Precipitation of China Meteorological Administration, Nanjing University of Information Science & Technology, Nanjing, China
*Corresponding author: waleabiye@gmail.com; eabiye@cerd.gov.ng

Received: January 07, 2016 **Accepted:** March 25, 2017

Abstract: This study presents an overview of near surface meteorological measurements carried out in a dense air-pollution plume environment of a scrap-iron recycling factory (7° 29'N, 4° 28'E, 262 m a.s.l) located at Ile-Ife, southwest Nigeria. This was done with a view to providing test meteorological dataset that could be used as input in advanced regulatory air pollution dispersion models. Gradient and single level continuous measurements of near surface atmospheric parameters comprising air temperature (1 and 5 m), relative humidity (1 and 5 m), global and net radiation fluxes (both at 1.5 m), soil heat flux (5 cm below surface), wind speed (1.5 and 5.5 m) and wind direction (5.5 m) were made between August 2012 and June 2014. The assay of sensors deployed includes two (2) pulse type cup anemometers (model A100ML), two (2) air temperature and relative humidity sensors (model HMP45), a potentiometer type wind vane (model W200P), a net radiometer (model NR-LITE), a pyranometer (model CS300), a soil heat flux plate (model HFP01) and a soil temperature probe (model T108). All the sensors for the measurement were instrumented to a 6 m meteorological mast and connected to a Campbell Scientific datalogger (model CR1000). The data obtained were sampled at 10 s resolution and stored as 10 min averages, later reduced to hourly averages. Generally, the location is characterized by daily mean air temperature (≥ 26°C), high relative humidity (RH > 70%) and weak winds (< 2.0 ms^{-1}). Hourly mean of net radiation reached a peak of 422.7, 382.0 and 477.0 Wm^{-2} in the years 2012, 2013 and 2014, respectively. On the other hand, hourly mean of soil heat flux reached a peak of 108.2, 93.2 and 119.2 Wm^{-2}, respectively for the same period. This high quality and extensive site-specific meteorological dataset would be useful for hands-on testing and deployment of air pollution dispersion models and for use in other environmentally related applications.

Keywords: Air temperature, dispersion models; net radiation, soil heat flux

Introduction

Indiscriminate release of harmful gaseous emissions from operations within the industrial sectors (e.g., scrap-iron recycling) into the atmosphere could constitute serious human health and environmental issues. This problem is exacerbated in Nigeria by lack of in-situ measurements of air pollutant and enforcement of guidelines that regulate short- and long-term impacts. There is also the problem of inadequate and improper control strategies caused by prohibitive costs of equipment and inadequate skilled manpower to monitor criteria air pollutants' concentration at all locations of interest.

An approach that has proven to be efficient and cost effective in obtaining estimates of the concentrations of these pollutants (e.g. SO_2, NO_X, CO, etc.) is the use of advanced regulatory (Gaussian-based) air pollution dispersion models. AERMOD, one of the most widely used regulatory air pollution dispersion model (Carruthers *et al.*, 2011; Nadoushan *et al.*, 2016) requires as input, basic meteorological variables to characterize the surface layer dynamical parameters that are needed in estimation of lateral (σ_y) and vertical dispersion (σ_z) coefficients, as well as pollutants' concentrations at downwind locations from a known source of atmospheric pollution. Unfortunately, the meteorological inputs required by the dispersion models are often compromised in the sense that location-specific measurements are not always available (Capelli *et al.*, 2013). As a consequence of this limitation, most atmospheric dispersion estimates of pollutants' concentrations are made from meteorological data obtained from sources different from the location of application thereby failing to fully represent the prevailing surface layer conditions at the required location. As such, the reliability of dispersion models' concentration estimates is strongly dependent on the representativeness of the input meteorological parameters to fully describe the atmospheric dynamics and surface layer characteristics at the source location (Pearce *et al.*, 2011).

Thus, providing regulatory air pollution dispersion model with site-specific, quality-assured surface layer meteorological data is therefore essential for obtaining plausible estimates of pollutants concentrations downwind from the released source. The basic routine meteorological measurements required include air temperature, relative humidity, wind speed and direction among others (Batterman *et al.*, 2010). This study was therefore carried out with a view to providing a less capital- and equipment-intensive methodology for reliable use of near surface meteorological data for possible application as input in advanced regulatory air pollution dispersion models.

Materials and Methods

Description of the study area

The study site (7° 29'N, 4° 28'E, 262 m a.s.l) is located at Fashina, Ile-Ife, a rural settlement in Ife-Central Local Government Area (LGA), Osun State, southwestern Nigeria (Fig. 1). Located off a high-traffic Ife-Ibadan expressway, Fashina is an agrarian community surviving on subsistence farming, animal husbandry and cottage industry like palm oil and cassava processing. A little distance inwards from the expressway, there are patches of declining cocoa plantation due to developmental encroachment of residential buildings. The road network in the area is unpaved except for the abandoned old Ife-Ibadan motorway. Generally, vehicular traffic in the interior areas is very low, being mostly plied by lorry tippers bearing sand and construction materials. Neighbouring communities around Fashina settlement include Ipetumodu and Akinlalu. The Obafemi Awolowo University Campus is about 7 km (as the crow flies) in the NE direction and the palace of the monarch, the Ooni of Ife, is about 8.5 km away in the East direction.

Climatologically, Fashina is located in the tropical wet and dry belt of West Africa. During the dry season, typically from November to February, the region is characterized by dry and dust-laden northeasterly winds, which have a long trajectory over the Sahara desert. Absence of wet deposition in dry season increases residence time of the dust in the atmosphere leading to a persistent haze, known locally as Harmattan. From March, which marks the transition period between dry and wet season, the southwesterly monsoon flow begins to move further inland bearing with it moisture-laden air mass from the coastal region. These two air masses (dry, dust-laden northeasterly and the moisture-laden southwesterly) meet over land at a zone of strong convergence referred to as Inter-Tropical Discontinuity (ITD). At the peak of wet season in July and August, maximum daytime air temperature ranges between 24.5 and 37.7^{o}C with the mean most times being about 26^{o}C. Daily mean relative humidity is between 59% and 87% (Jegede *et al.*, 2004). Seasonal changes are associated with north-south movement of the ITD line. At about latitude 7 ^{o}N, the ITD position varies between 5 ^{o}N in January and about 14 ^{o}N in June. The predominant surface wind at the location is southwesterly virtually all year round due to nearness to the ITD southernmost position.

A scrap-iron recycling factory is sited across the expressway, southwest of the study area (Fig. 1). The scrap-iron recycling factory is a private smelter facility and it is the only industrial activity within a radius of 20 km. It is situated on a land area of about 500 by 500 m (256 m a.s.l). As a mini-mill, the factory depends hundred percent on scrap metals (Owoade *et al.*, 2011; Owoade *et al.*, 2013) which are supplied from time to time by commercial truck owners and small scale individual scrap scavengers. A dumpsite with massive deposit of slag from the recycling process is located behind the recycling factory.

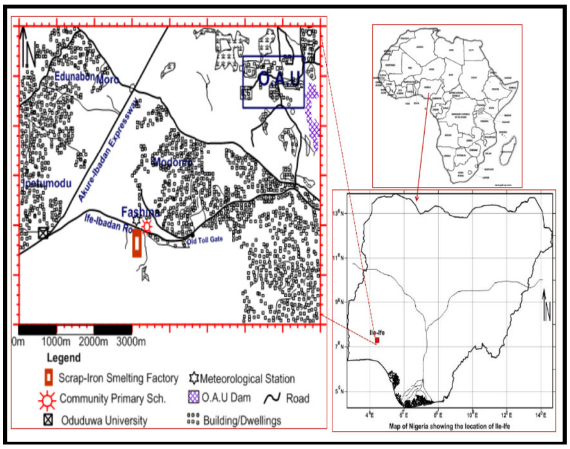

Fig. 1: Map Showing Fashina, the measurement location (7^{o} 29’ N; 4^{o} 28’ E) in Ile-Ife, Southwestern Nigeria.

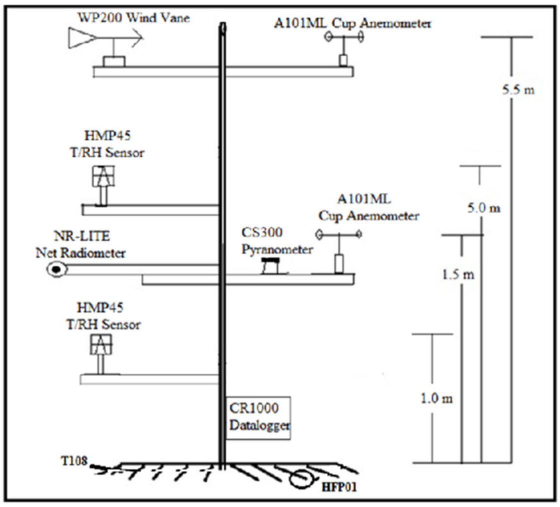

Fig. 2: Schematic diagram of sensors’ positioning on the 6-m meteorological mast at Fashina, study site.

Measurements of meteorological parameters

A 6-m meteorological mast (the schematic is shown in Fig. 2) was installed at the measurement site, approximately 200 m away from the factory in the northern direction. The immediate surroundings of the measurement site has leveled ground surface moderately overgrown with short grasses and was well maintained throughout the study period. Topography of the area is flat. Land use pattern in the vicinity of the mast comprises of sparsely grown cassava and maize farmlands, and patches of uncultivated plots with few scattered trees. The location was chosen such that measurements from the station depict actual meteorological conditions at the location. The mast, a 2.5-inch antirust-coated pipe designed to support booms at three different levels and oriented in a west-east direction, was instrumented for measurements of routine near surface micrometeorological parameters. This was with a view to obtaining site-specific meteorological dataset required as input in dispersion models for estimating concentrations of gaseous emissions released from the recycling factory.

In August 2012, the mast was instrumented with two (2) pulse type cup anemometers (model A100ML), two (2) air temperature and relative humidity sensors (model HMP45), a potentiometer type wind vane (model W200P), a net radiometer (model NR-LITE), a pyranometer (model CS300), a soil heat flux plate (model HFP01) and a soil temperature probe (model T108). A schematic diagram of the placement heights for the sensors is as shown in Fig. 2 while the positioning and specifications of the sensors are summarized in Table 1. The measurement levels for wind (1.5 and 5.5 m), temperature and relative humidity (both at z_1 = 1 m and z_2 = 5 m) were so chosen such that the ratio z_2/z_1 falls within ~ 4 - 8 (Arya, 2001; Foken, 2008) to ensure that the gradients of wind, temperature and relative humidity are sufficient for obtaining appreciable flux values to resolve the surface layer parameters.

Table 1: Specifications of the sensors used for measurement

Parameter	Instrument	Manufacturer (Model)	Accuracy/ Sensitivity	Heights (m)
Wind Speed	Cup Anemometer (2)	Vector Instruments, UK (A101ML)	Dist. const. 2.3m (Threshold 0.15ms^{-1})	1.5 & 5.5
Wind Direction	Potentiometer Wind Vane	Vector Instruments, UK (WP200)	±3°	5.5
Air Temperature & Relative Humidity	Temperature and Relative Humidity Sensor (2)	Campbell Scientific, USA (HMP45)	±0.4°C ±2% (0 – 90%) & ±3% (90 – 100%)	1.0 & 5.0
Net Radiation	Net Radiometer	Campbell Scientific, USA (NR-LITE)	10μ V/(Wm^{-2})	1.5
Global Radiation	Pyranometer	Kipp and Zonen, Netherlands (CS300)	± 5%	1.5
Soil Heat Flux	Heat Flux Plate	Huksefux (HFP01)	~ 50μ V/W.m^{-2}	5 cm below surface
Soil Temperature	Soil Temperature Probe	Campbell Scientific, USA (T108)	±0.05°C	5 cm below surface

Fig. 3: Plume release scenario (a) idle period; (b) commencement of operation; (c) peak of smelting operation; and (d) during the field measurement; at the scrap-iron recycling plant located at Fashina, Ile-Ife, Ife Central Local Government Area, Southwestern Nigeria.

Data acquisition and analysis

Data acquisition commenced in August 2012 and continued till June 2014 when the experimental field measurements were concluded. Meteorological data were available for all the period of the measurements except for the months of January to March in 2013 when the station was temporarily shut down for maintenance purposes. The sensors were connected to a Campbell Scientific datalogger (model CR1000), which served as a measurement and control module, and configured to measure meteorological parameters every 10 sec. and stored as 1 min averages except for the wind direction that was sampled at 10 min intervals. Data for all the parameters measured were carefully checked for instrumental errors and out-range values. Quality assurance and quality control (QA/QC) procedure were then carried out on the entire dataset to ensure its physical reliability. Data points with spurious or missing values were either removed or replaced using interpolation method where necessary. Collected data were then processed into sequential hourly averages. These were later reduced to monthly averages. The wind direction was reduced using the methodology recommended for meteorological monitoring in regulatory modeling applications (USEPA, 2000).

Results and Discussions

Monthly diurnal variation of measured air temperature, relative humidity, net radiation flux, soil heat flux, soil temperature and wind speed at the study location for the year 2012 are presented in Fig. 4(a) – (e), respectively. Since the measurements started in August 2012, data obtained for this month were not used to ensure consistency and avoid errors. For the month of September 2012, the hourly mean values of air temperature increased from 22.4°C just before dawn (about 05:00LT) and as the sun rises, the values increased monotonically to reach a maximum value of 27.9°C at about 15:00 LT. Thereafter, the air temperature values dropped as the sun sets. The daily mean air temperature obtained for the month was 24.6°C (Fig. 4a). The relative humidity (RH) values varied between a minimum value of 69.3% at about 15:00 LT and a maximum value of 92.2 % at night. The mean relative humidity obtained for the month was 84.1%. The high values of RH ~ 90 % at night time indicated a near saturated atmosphere (Fig. 4b).

This is attributable to the prevailing southwesterly current of maritime origin, which is moist-laden. The values of net radiation from midnight to about 7:00 LT were negative and fairly constant with values ranging between -31.9 and -11.4 Wm^{-2} (Fig. 4c). This indicated there was radiative cooling at the surface during this period. Beyond 7:00 LT, the net radiation turned to positive values and increased steadily as the sun rises overhead to reach a maximum value of 377.2 Wm^{-2} which occurred at about 14:00 LT. The soil heat flux reached its minimum value of -36.8 Wm^{-2} at 20:00 LT and maximum values of 99.8 Wm^{-2} at 13:00 LT, respectively (Fig. 4c). Daytime values of soil heat flux were found to be between 0.1 - 0.26 of the net radiation values. This values fall within the range 0.13 - 0.3 of net radiation quoted in the literatures (Jegede, 1997; Ayoola *et al*., 2014). The difference between net radiation and soil heat flux represent the amount of energy, in form of sensible and latent heat flux, available for heat and mass transfer at the surface, and consequently to drive pollutants mixing. The maximum value recorded for soil temperature was 30.9°C (Fig. 4d). The hourly mean values of wind speed showed a diurnal pattern, increasing from a minimum of 0.7 ms^{-1} in the early morning (around 06:00 LT) to reach a peak value of 1.8 ms^{-1} by the late afternoon (around 15:00 LT). The mean wind speed value recorded at the site for September 2012 was 1.3 ms^{-1} (Fig. 4e). This suggests that low-level flow was weak at the study location during the period of observation. This low wind speed value is typical of the low latitudes (tropical areas). High values of wind speed only occur during storms or disturbed weather. The daily mean air temperature obtained for the month of October 2012 was 25.1°C while the maximum air temperature attained was 35.5°C around 16:00 LT. (Fig. 4a). Since the month represents a transition between the wet and dry season for the measurement location, it is usually associated with changes in southwesterly to northeasterly flows. It is of high significance to air pollution dispersion because as the surrounding becomes warmer, it enhances the capacity of the atmosphere to exchange air parcels through convective processes and buoyancy effects. It thus indicates that pollutants are dispersed further away from the source in this month than the previous one. The relative humidity on the other hand reached a minimum value of 62.9% at about 15:00 LT and a maximum value of 93.1% at night. The mean value was 82.8% (Fig. 4b). The high relative humidity observed in the early morning hours and at nighttime plays an important role in moderating the residence time of gaseous and particulate pollutants in the atmosphere and consequently pollutants concentration levels. In a study by Elminir (2007), it was established that atmospheric pollutants' concentration decreases with increase in relative humidity and vice versa. This is so because as the relative humidity increases, pollutant particles absorb more water. The absorbed water increases the size and volume of the particle thus the particles become denser and easily deposited to the surface (Zhang *et al*., 1993). For the net radiation, a slight dip in the value of the net radiation between 10:00 and 12:00 LT was observed (see Fig. 4c). This dip is a common phenomenon in tropical humid region and can be attributed to the effect of cloud drifts that blocks out incoming solar radiation. The maximum value of net radiation observed for this month was higher (90.0 Wm^{-2}) than for the previous month. The daytime values of the soil heat flux were found to be between 0.10 and 0.26 of the net radiation. This is found to be almost the same as that of September 2012. Maximum value recorded for soil temperature was 37.0°C. This was greater than the value recorded for the previous month (Fig. 4d). The mean wind speed recorded at the site for the month was 1.2 ms^{-1}. During periods of atmospheric stagnation that is associated with low wind speeds $\bar{u} < 1.0$ ms^{-1} (Richard *et al*., 1994), wind-induced horizontal mixing of pollutants is suppressed. Thus, pollutants concentrations increase near the emitting source. In the areas surrounding the scrap-iron smelting factory, visibility will be greatly reduced at such periods of low winds especially early in the morning (about 05:00 LT). Thus, the low wind speed obtained at the study site may increase atmospheric pollutants' concentrations and affect visibility in the vicinity of the scrap-iron recycling factory especially during period of continuous release of gaseous emission.

For the month of November 2012, the air temperature minimum was 23.3°C while the maximum was 31.2°C around 16:00 LT. These values were higher than those of the previous month. The daily mean air temperature obtained for the month was 26.1°C (Fig. 4a). The relative humidity values varied between a minimum of 57.6% at about 16:00 LT and a maximum of 92.5% at about 06:00 LT. The mean relative humidity obtained for the month was 80.4% (Fig. 4b). The maximum value of the net radiation for the month was 455.8 Wm^{-2} at 14:00 LT while that of the soil heat flux was 114.7 Wm^{-2} at the same time (Fig. 4c). The maximum value of soil temperature recorded for this month was greater than that of the two previous months (i.e. 39.7°C) (Fig. 4d). Daytime values of soil heat flux were found to be between 0.14 and 0.29 of the net radiation values. The peak value of mean wind speed was 1.6 ms^{-1} by the late afternoon (around 14:00 LT) while the mean wind speed values recorded at the site for the month was 1.0 ms^{-1}.

For the month of December 2012, the maximum value of the air temperature recorded was 31.7°C at about 16:00 LT with the daily mean being 26.9°C (Fig. 4a). The relative humidity minimum and maximum recorded were 51.8% at about 16:00 LT and 91.7% at about 06:00 LT, respectively. The mean relative humidity obtained for the month was 77.7%. This was observed to be lower than the mean relative humidity values obtained for September (84.1%) and October (82.8%). The maximum value of the net radiation was 404.8 Wm^{-2} around 14:00 LT with the daily mean value being 76.4 Wm^{-2} (Fig. 4c). The soil heat flux reached a maximum value of 101.1 Wm^{-2} at 14:00 LT while the daytime values of the soil heat flux was between 0.18 and 0.34 of the net radiation values (Fig. 4c). The maximum soil temperature recorded for the year was 41.3°C (Fig. 4d). The maximum value of the wind speed was 1.5 ms^{-1}. This was the highest daily mean value recorded for the year 2012. This implied that surface wind speeds were relatively stronger in this month compared to other months (September - December) in 2012. High wind speed significantly affects plume rise and ground-level concentrations because plume rise are negligible at very high wind speeds and the effective stack height may also be reduced (Beychock, 2005). When this occurs, the plume may be brought to the ground at downwind locations not far from the source. However, due to the increased volume of air associated with increasing wind speeds, ground-level concentrations are usually reduced. As the wind speed increases in December, plume rise and the effective stack height may be reduced thus suggesting that ground-level concentrations of pollutants are lower compared to other months. The summaries of the hourly variables are presented in Table 2.

Figure 5 shows the various parameters of air temperature, relative humidity, net radiation, soil heat flux, soil temperature and wind speed for the months of March to December in the year 2013. Maximum air temperature recorded for the month of March 2013 was 32.0°C while the mean for the month was 26.9°C (Fig. 5a). The maximum relative humidity on the other hand was 90.1%

with the mean being 76.9% (Fig. 5b). This month represents a transition from dry season to wet one with high probability of reducing atmospheric dispersion of gaseous emissions from the scrap-iron recycling factory depending on the strength of the horizontal wind speed. This can be attributed to decrease in air temperature and consequent reduction in convective exchange at the surface. The maximum values of the net radiation and soil heat flux were 546.9 Wm^{-2} and 125 Wm^{-2}, respectively (Fig. 5c). The mean values of the net radiation and soil heat flux, on the other hand, were 120.1 Wm^{-2} and 6.7 Wm^{-2}, respectively (Fig. 5c). The maximum value of the soil temperature (shown in Fig. 5d) was 36.6^{o}C while its mean value was 31.0^{o}C. The maximum wind speed recorded for the month was 0.5 ms^{-1} with its mean value being 0.2 ms^{-1}. The maximum air temperature recorded for the month of April 2013 was 31.2^{o}C while the mean for the month was 26.4^{o}C (Fig. 5a). This was slightly greater than the value for the previous month. The relative humidity maximum on the other hand was 91.8% with the mean being 78.7% (Fig. 5b). The maximum values of the net radiation and soil heat flux were 515.5 and 88 Wm^{-2}, respectively (Fig. 5c). The mean value of the net radiation, on the other hand, was 111.8 Wm^{-2} (Fig. 5c). The maximum value of the soil temperature (shown in Fig. 5d) was 34.0^{o}C while its mean value was 29.7^{o}C. These values are slightly lower than the previous month. The maximum wind speed recorded for the month was 2.1 ms^{-1} with its mean value being 1.2 ms^{-1}.

For the year 2013, the least of the maximum air temperature recorded occurred in the month of August with a value of 28.1^{o}C while the mean value recorded was 23.5^{o}C (Fig. 5a). The range of values obtained between May and December 2013 for air temperature, relative humidity, net radiation, soil heat flux and wind speed were 21.4 – 31.8^{o}C, 43.6 – 94.5%, -54.7 – 477.7 Wm^{-2}, -56.7 – 133.5 Wm^{-2} and 0.1 – 2.2 ms^{-1}, respectively. A bimodal trend was observed in the air temperature, soil temperature, net radiation and the soil heat flux parameters in 2013. The summary of the hourly variables is presented in Table 3.

Table 2: Hourly mean values of meteorological parameters at the study site for 2012

LT (GMT+1)	WS (ms^{-1})	T (^{o}C)	RH (%)	NR (Wm^{-2})	SHF (Wm^{-2})
01	1.0	23.6	90.9	-23.6	-35.2
02	0.9	23.4	91.4	-19.6	-33.2
03	0.8	23.4	91.8	-18.0	-31.4
04	0.8	23.3	92.1	-17.7	-30.2
05	0.7	23.2	92.3	-17.9	-29.8
06	0.7	23.2	92.4	-17.2	-28.8
07	0.7	23.2	92.3	-15.0	-27.6
08	0.7	23.4	92.1	11.7	-19.8
09	1.2	24.1	89.3	70.4	0.5
10	1.4	25.2	83.9	158.9	26.2
11	1.6	26.4	77.7	255.2	54.9
12	1.6	27.3	72.0	326.7	78.1
13	1.7	28.6	67.0	416.8	102.2
14	1.8	29.5	63.4	422.7	108.2
15	1.8	30.0	61.1	370.1	98.4
16	1.8	30.2	60.6	275.3	74.7
17	1.8	29.8	62.8	137.7	34.6
18	1.6	28.6	68.3	18.1	-5.7
19	1.4	27.1	76.3	-34.4	-30.1
20	1.3	25.9	81.3	-38.1	-39.2
21	1.4	25.1	85.1	-34.8	-40.2
22	1.3	24.5	87.3	-31.1	-39.5
23	1.3	24.1	89.1	-28.0	-38.4
24	1.1	23.9	90.2	-24.7	-36.0

LT = Local Time; **WS** = Wind Speed; **T** = Temperature; **RH** = Relative Humidity; **NR** = Net Radiation; **SHF** = Soil Heat Flux

Table 3 Hourly mean values of meteorological parameters at the study site for the year 2013

LT (GMT+1)	WS (ms^{-1})	T (^{o}C)	RH (%)	SHF (Wm^{-2})	NR (Wm^{-2})
01	0.5	22.8	94.3	-33.9	-26.7
02	0.4	22.7	94.7	-32.5	-24.9
03	0.4	22.5	94.9	-31.5	-24.2
04	0.3	22.4	95.1	-30.6	-23.9
05	0.3	22.3	95.4	-29.6	-23.2
06	0.2	22.3	95.5	-29.0	-22.9
07	0.2	22.2	95.5	-27.6	-19.8
08	0.3	22.6	95.4	-16.9	6.6
09	0.5	23.5	92.7	7.4	62.4
10	0.8	24.7	85.9	35.2	152.0
11	1.0	26.0	78.5	62.8	245.6
12	1.1	27.1	72.7	84.4	318.2
13	1.1	27.9	68.7	93.2	379.1
14	1.1	28.6	66.0	92.6	382.0
15	1.2	29.0	64.4	83.5	362.3
16	1.2	29.1	64.3	63.6	298.7
17	1.2	28.6	66.9	22.8	163.8
18	1.1	27.5	72.3	-12.0	47.8
19	0.7	25.8	80.1	-35.0	-23.7
20	0.7	24.6	86.2	-40.8	-39.6
21	0.8	24.0	89.4	-40.6	-35.7
22	0.7	23.5	91.5	-39.2	-32.8
23	0.6	23.2	93.0	-37.0	-30.8
24	0.6	23.0	93.8	-35.3	-28.2

LT = Local Time; **WS** = Wind Speed; **T** = Temperature; **RH** = Relative Humidity; **NR** = Net Radiation; **SHF** = Soil Heat Flux

Table 4: Hourly mean values of meteorological parameters at at the study site for the year 2014

LT (GMT+1)	WS (ms^{-1})	T (^{o}C)	RH (%)	SHF (Wm^{-2})	NR (Wm^{-2})
01	0.5	24.1	94.9	-37.3	-38.2
02	0.4	23.8	96.3	-36.7	-36.5
03	0.3	23.6	97.1	-35.4	-35.0
04	0.3	23.4	97.7	-34.6	-33.2
05	0.3	23.3	97.7	-33.9	-31.8
06	0.3	23.2	98.1	-32.9	-30.8
07	0.2	23.1	98.4	-31.9	-28.7
08	0.3	23.4	98.3	-23.2	-1.8
09	0.5	24.5	95.7	1.3	69.5
10	0.8	26.2	86.3	31.6	182.5
11	1.0	27.9	74.0	68.0	305.7
12	1.3	29.4	64.6	95.0	379.5
13	1.3	30.7	57.8	113.8	444.4
14	1.5	31.8	52.8	119.2	477.0
15	1.5	32.4	50.0	106.1	431.1
16	1.5	32.7	48.3	78.7	330.5
17	1.4	32.4	49.9	39.5	193.0
18	1.3	30.9	56.1	-6.0	44.7
19	1.0	28.9	65.4	-34.7	-34.9
20	0.9	27.1	74.3	-44.4	-49.7
21	1.0	26.0	80.2	-43.9	-48.2
22	0.9	25.3	85.3	-42.5	-45.4
23	0.7	24.8	89.8	-40.3	-42.8
24	0.6	24.4	92.8	-38.1	-39.4

LT = Local Time; **WS** = Wind Speed; **T** = Temperature; **RH** = Relative Humidity; **NR** = Net Radiation; **SHF** = Soil Heat Flux

Table 5: Mean values of the meteorological parameters for the entire study period (September, 2012 to June, 2014)

LT (hr)	T (°C)	RH (%)	NR (Wm^{-2})	SHF (Wm^{-2})	WS (ms^{-1})
Jan	26.4	77.1	68.2	6.7	0.6
Feb	27.4	68.6	81.3	10	0.7
Mar	27.5	77.5	107.3	32.9	1.0
Apr	26.6	82.3	116.8	9.3	1.0
May	26.1	84.7	113.8	2.5	0.8
Jun	25.1	84.1	81.7	-0.5	0.8
Jul	24.0	86.5	81.7	0.5	0.9
Aug	23.7	86.3	55.4	2.6	0.8
Sept	24.6	86.3	88.2	4.9	0.9
Oct	25.0	85.5	101.4	6.1	0.8
Nov	26.1	81.5	94.3	5.5	0.5
Dec	25.9	77.2	83.6	2.5	0.4
Wet	**25.0**	**85.1**	**91.3**	**2.4**	**0.9**
Dry	**26.7**	**76.38**	**86.9**	**11.5**	**0.6**
Period	**25.7**	**81.5**	**89.5**	**6.2**	**0.8**

LT = Local Time; **WS** = Wind Speed; **T** = Temperature; **RH** = Relative Humidity; **NR** = Net Radiation; **SHF** = Soil Heat Flux

Shown in Fig. 6 are the various parameters of air temperature, relative humidity, net radiation, soil heat flux, soil temperature and wind speed for the months of January to May in the year 2014. The observed diurnal trends for these parameters were similar to those observed in the previous year. The range of values obtained between January and May 2014 for air temperature, relative humidity, net radiation, soil heat flux and wind speed were 22.9 – 33.6°C, 33.2 – 93.9%, -57.8 – 533.8 Wm^{-2}, -51.6 – 146.4 Wm^{-2} and 0 – 2.2 ms^{-1}, respectively. In addition, the summary of the hourly variables is summarized in Table 4.

In general, for the three years considered, the air temperature increased as incoming solar radiation from the sun warms up the land and in turn, the air near the surface, first by conduction and then convection. Thus, in response to the energy input from the sun, the air temperature increases until about local noon (13:00LT) when the sun is directly overhead and the solar intensity reaching the surface is at its maximum. It is understood that increase or decrease in air in air temperature with height plays an important role in determining the stability of the atmosphere i.e. lapse rate, and consequently, its capacity to disperse pollutants concentration. Hence, the daytime is typically unstable and night time/evening periods are stable. Lapse rate calculated for the location around 13:00 was – 0.12°C/m. Periods with large lapse rate values such as this will have greater dispersion and dilution of pollutants concentrations because the atmosphere is extremely unstable, lapse rate < -0.0189°C/m (Jegede *et al.*, 1997; Beychock, 2005). This can be linked with increased vertical turbulence due to rising thermals that drives the exchange (downdraft and updraft) of pollutants particles between the surface and the atmospheric boundary layer. As a result of the intense mixing of the atmospheric boundary layer, levels of concentration of atmospheric pollutants will be reduced during the daytime but high at nighttime. In general, weather regimes with high daily mean air temperature (≥ 26.0°C) are known to have better air quality due to increased convective turbulence and enhanced buoyancy of air pollutants than on days with lower air temperature (Buchholz *et al.*, 2010).

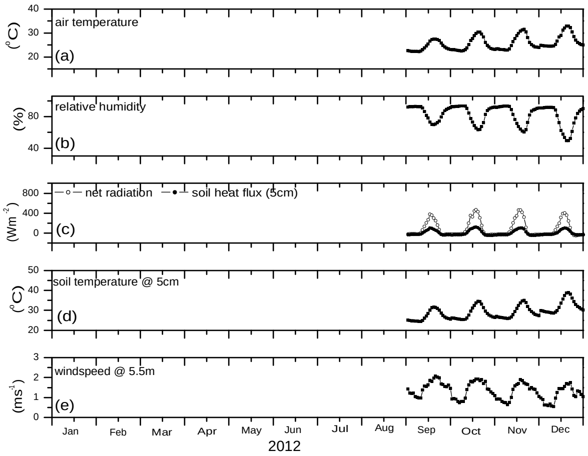

Fig. 4: Diurnal variations of (a) air temperature; (b) relative humidity; (c) net radiation and soil heat flux; (d) soil temperature and (e) wind speed at the study site for 2012.

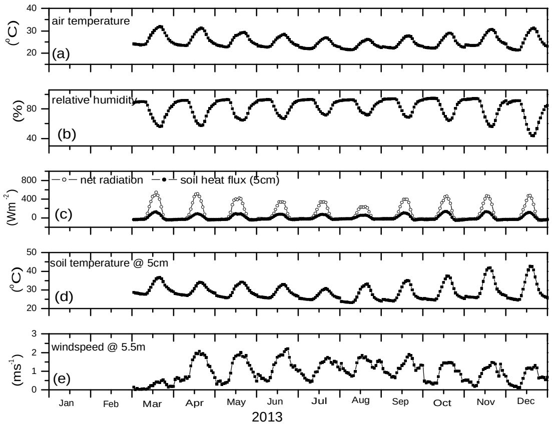

Fig. 5: Diurnal variations of (a) air temperature; (b) relative humidity; (c) net radiation and soil heat flux; (d) soil temperature and (e) wind speed at the study site for 2013.

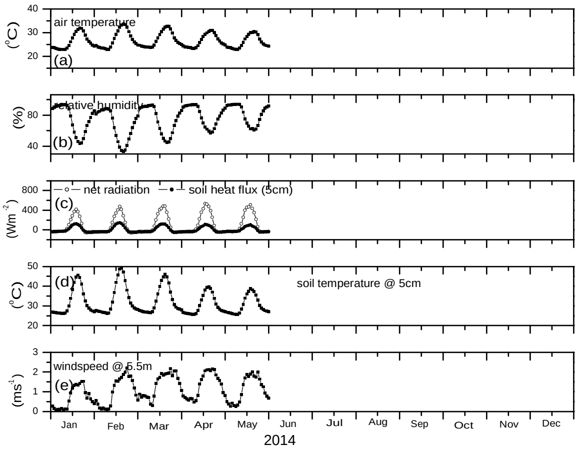

Fig. 6: Diurnal variations of (a) air temperature; (b) relative humidity; (c) net radiation and soil heat flux; (d) soil temperature and (e) wind speed at the study site for 2014.

Due to the high moisture content of the prevailing air current, the conditions will promote coagulation of suspended particulate matter as a result of their hygroscopic nature. As such, gaseous emissions may be removed by wet deposition thus leading to its reduced concentration at downwind locations from the scrap-iron recycling factory. Also, the high relative humidity (RH) observed during early morning hours and at night time has significant implication on visibility in the immediate environment of the scrap-iron recycling factory. During the period of RH > 70%, hygroscopic particles take up moisture and increase in size. The increase in size of such hygroscopic pollutants increases their scattering coefficient for light. Since visibility is inversely proportional to the scattering coefficient, high relative humidity thus leads to reduced visibility. On the other, periods of low RH (observed to occur in the afternoon between 12:00 – 13:00 LT) can be associated with good visibility. At night time, the high values of relative humidity obtained in this study indicated the possibility for the occurrence of precipitation, which in turn would reduce atmospheric pollutants concentration through wash-out. Precipitation processes are often accompanied by in-cloud scavenging of suspended particles and gases in the air, which in turn results in lowered pollutant concentrations (Kasper and Puxbaum, 1998).

The weak winds prevalent in the study location will promote incidences of elevated concentration of atmospheric pollutants especially in the early morning period when the wind speed is lowest and relative humidity is high. Thus, pollutants concentrations around this period are expected to be at the lowest values. The summary of the hourly variables is given in Table 5. For the net radiation, it is observed that there was a time lag of about one hour between the time of occurrence of maximum of net radiation (13:00 LT) and air temperature (14:00 LT). The time lag is due to delay for the surface to respond to the direct heating by the sun.

Conclusion

This study has provided quality-assured and site-specific meteorological measurement in the vicinity of a scrap-iron recycling factory located at Fashina, Ile-Ife, Southwestern Nigeria. The approach used in the study is a less capital- and equipment-intensive methodology for the acquisition of routine meteorological data which can be used as input in advanced regulatory air pollution dispersion models. This dataset provided a baseline, in the study area, useful for testing air pollution dispersion models, estimating concentrations of air pollutants in the vicinity of the site using Gaussian-based air pollution dispersion model, and in identifying the areas prone to the elevated concentrations of gaseous emissions in the vicinity of operations of the recycling plant.

Conflict of Interest

No potential conflict of interest was reported by the authors.

Acknowledgement

The authors are grateful for the financial support, meteorological sensors and human resources provided by the Atmospheric Physics Research Group (APRG, led by Prof. O. O. Jegede) in the Department of Physics and Engineering Physics, Obafemi Awolowo University, Ile-Ife, Nigeria.

References

Arya SP 2001. Introduction to Micrometeorology. Academic Press. San Diego, Califonia, USA, p. 420.

Ayoola MA, Sunmonu LA, Bashiru MI & Jegede OO 2014. Measurement of net-all wave radiation at a tropical location, Ile-Ife, Nigeria. *Atmosfera.*, 27(3): 305 - 315.

Batterman SA, Zhang K & Kononowech R 2010. Prediction and analysis of near-road concentrations using a reduced-form emission/dispersion model. *Environmental Health*

Beychok MR 2005. Fundamentals of Stack Gas Dispersion. Irvine, Newport Beach, CA, USA, Fourth Edition, p. 201.

Buchholz S, Junk J, Krein A, Heinemann G & Hoffmann L 2010. Air pollution characteristics associated with mesoscale atmospheric patterns in northwest continental Europe. *Atmos. Environ.*, 44: 5183 -5190.

Capelli L, Sironi S, Del Rosso R & Guillot J 2013. Measuring odours in the environment vs. dispersion modelling: A review. *Atmos. Environ.*, 79: 731–743.

Carruthers DJ, Seaton MD, McHugh CA, Sheng X, Solazzo E, Vanvyve EJ 2011. Comparison of the complex terrain algorithms incorporated into two commonly used local-scale air pollution dispersion models (ADMS and AERMOD) using a hybrid model. *Air Waste Manag Assoc.,* 61(11): 1227 – 1235.

Elminir HK 2007. Relative influence of air pollutants and weather conditions on solar radiation part 1: relationship of air pollutants with weather conditions. *Meteorol. Atmos. Phys.*, 96: 245 - 256.

Foken T 2008. Micrometeorology. Springer-Verlag Berlin Heidelberg, Germany, p. 320.

Jegede OO, Mauder M, Okugbue EC, Foken T, Balogun EE, Adedokun AA, Oladiran EO, Omotosho JA, Balogun AA, Oladosu OR, Sunmonu LA, Ayoola MA, Aregbesola TO, Ogolo EO, Nymphas EF, Adeniyi MO, Olatona GI, Ladipo KO, Ohamobi SI, Gbobaniyi EO & Akinlade GO 2004. The Nigerian Micrometeorological Experiment (NIMEX): An Overview. *Ife J. Sci.*, 6(2): 191 - 202.

Jegede OO, Fasheun TA, Adeyefa ZD & Balogun AA 1997. The effect of atmospheric stability on the surface-layer characteristics in a low-wind area of tropical West Africa, *Bound. Layer Meteor*., 85: 309 – 323.

Kasper A & Puxbaum H 1998. Seasonal variation of SO_2, HNO_3, NH_3 and selected aerosol components at Sonnblick (3106 m a.s.l.). *Atmos. Environ.*, 32(23): 3925 - 3939.

Nadoushan NAM, Mansouri N & Nezhadkurki F 2016. Assessment of AERMOD model's sensitivity to terrain features for identifying air pollutants receptor points in steel industry. *J. Fundam. Appl. Sci.*, 8(3S): 1399-1413.

Owoade OK, Jegede OO, Ayoola MA, Fawole OG, Bashiru MI, Olise FS & Ogundele LT 2013. Concentrations of particulate matter from an iron and steel smelting plant located along a busy high way in southwestern Nigeria. *Ife J. Sci.*, 15(1): 31 – 39.

Owoade OK, Olise FS, Olaniyi HB, Obioh IB & Bolzacchini E 2011. Mass and energy audit in a Nigerian iron and steel smelting factory: An operational and efficiency study. *Ife J. Sci.*, 13(1): 133 – 142.

Pearce JL, Beringer J, Nicholis N, Hyndman RJ & Tapper NJ 2011. Quantifying the influence of local meteorology on air quality using generalized additive models. *Atmos. Environ.*, 45(6): 1328 – 1336.

Richard WB, Donald LF, Tuner DB & Arthur CS 1994. Fundamentals of Air Pollution. Academic Press, London, p. 574.

USEPA 2000. Meteorological Monitoring Guidance for Regulatory Modeling Applications. EPA-454/R-99-005 Office of Air Quality Planning and Standards Emissions Monitoring and Analysis Division Research Triangle Park, North Carolina.

Zhang XQ, McMurry PH, Hering SV & Casuccio GS 1993. Mixing characteristics and water content of submicron aerosols measured in Los Angeles and at the Grand Canyon. *Atmos. Environ.*, 27(10): 1593 - 1607.